

# Additional attenuation of natural VLF electromagnetic waves observed by the DEMETER spacecraft resulting from preseismic activity

David Píša, František Němec, Ondřej Santolík, Michel Parrot, Michael Rycroft

► **To cite this version:**

David Píša, František Němec, Ondřej Santolík, Michel Parrot, Michael Rycroft. Additional attenuation of natural VLF electromagnetic waves observed by the DEMETER spacecraft resulting from preseismic activity. *Journal of Geophysical Research Space Physics*, American Geophysical Union/Wiley, 2013, 118, pp.5286-5295. 10.1002/jgra.50469 . insu-01179327

**HAL Id: insu-01179327**

**<https://hal-insu.archives-ouvertes.fr/insu-01179327>**

Submitted on 22 Jul 2015

**HAL** is a multi-disciplinary open access archive for the deposit and dissemination of scientific research documents, whether they are published or not. The documents may come from teaching and research institutions in France or abroad, or from public or private research centers.

L'archive ouverte pluridisciplinaire **HAL**, est destinée au dépôt et à la diffusion de documents scientifiques de niveau recherche, publiés ou non, émanant des établissements d'enseignement et de recherche français ou étrangers, des laboratoires publics ou privés.

## Additional attenuation of natural VLF electromagnetic waves observed by the DEMETER spacecraft resulting from preseismic activity

David Piša,<sup>1,3</sup> František Němec,<sup>2</sup> Ondřej Santolík,<sup>1,2</sup> Michel Parrot,<sup>3</sup> and Michael Rycroft<sup>4</sup>

Received 29 March 2013; revised 13 June 2013; accepted 22 July 2013; published 16 August 2013.

[1] We use VLF electromagnetic wave data measured by the DEMETER (Detection of Electro-Magnetic Emissions Transmitted from Earthquake Regions) satellite at an altitude of about 700 km to check for the presence of statistically significant changes of natural wave intensity (due to signals from lightning) related to preseismic activity. All the relevant data acquired by DEMETER during almost 6.5 years of the mission have been analyzed using a robust two-step data-processing schema. This enables us to compare data from the vicinity of about 8400 earthquakes with an unperturbed background distribution based on data collected during the whole DEMETER mission and to evaluate the statistical significance of the observed effects. We confirm previously reported results of a small but statistically significant decrease of the wave intensity (by  $\sim 2$  dB) at frequencies of about 1.7 kHz. The effect is observed for a few hours before the times of the main shocks; it occurs during the night. The effect is stronger between March and August, at higher latitudes and for the positions of hypocenters below the sea. We suggest an explanation based on changed properties of the lower boundary of the ionosphere, which leads to a decrease of the intensity of lightning-generated whistlers observed at the spacecraft altitude. This effect might result from a lowering of the ionosphere associated with an increase in the electrical conductivity of the lower troposphere due to an additional ionization of air molecules at the Earth's surface prior to earthquakes.

**Citation:** Piša, D., F. Němec, O. Santolík, M. Parrot, and M. Rycroft (2013), Additional attenuation of natural VLF electromagnetic waves observed by the DEMETER spacecraft resulting from preseismic activity, *J. Geophys. Res. Space Physics*, 118, 5286–5295, doi:10.1002/jgra.50469.

### 1. Introduction

[2] Over the past 20 years, considerable progress has been made in the field of seismo-electromagnetic effects. The main aim of this study is to look for possible short-term precursors of earthquakes ( $\sim$ hours) that would allow us to predict these devastating events. Although various types of possible ionospheric precursors have been reported (e.g., changes in temperature, plasma density, or conductivity), electromagnetic perturbations are probably one of the most promising candidates. These perturbations have been observed both using ground-based measurements and satellites. They are believed to occur over a wide range of frequencies, from direct current to very high frequency [Larkina *et al.*, 1989; Tate and Daily, 1989; Serebryakova

*et al.*, 1992; Molchanov *et al.*, 1993; Parrot, 1994a, 1994b; Asada *et al.*, 2001; Hattori, 2004; Hobara and Parrot, 2005; Bortnik *et al.*, 2008; Němec *et al.*, 2008, 2009; Piša *et al.*, 2012]. Nevertheless, it is very difficult to identify these effects in the ionosphere, because the amplitude of the earthquake-related perturbations is much lower than the amplitude of natural variations due to other sources. In fact, there is still a controversy concerning the very existence of seismo-electromagnetic effects [Henderson *et al.*, 1993; Rodger *et al.*, 1996; Clilverd *et al.*, 1999; Thomas *et al.*, 2009a, 2009b]. On the other hand, there are many theories that attempt to describe physical processes before earthquakes and which try to explain why these precursors may occur. A review of these processes can be found in Pulinets and Boyarchuk [2004], Freund [2011], and the references therein. A process that can explain many observations is based on the emission of a radioactive gas or metallic ions before an earthquake [e.g., Sorokin *et al.*, 2001], which may change the distribution of electric potential above the surface of the Earth and then up to the ionosphere. Penetration of the electric field to the ionosphere could induce anomalies in the ionospheric plasma density and/or conductivity, which are observed above seismic zones [see e.g., Liu *et al.*, 2006; Kon *et al.*, 2011]. Harrison *et al.* [2010] proposed that radon emitted before an earthquake would increase the

<sup>1</sup>Institute of Atmospheric Physics AS CR, Prague, Czech Republic.

<sup>2</sup>Faculty of Mathematics and Physics, Charles University in Prague, Prague, Czech Republic.

<sup>3</sup>LPC2E/CNRS, Orléans, France.

<sup>4</sup>CAESAR Consultancy, Cambridge, UK.

Corresponding author: D. Piša, Institute of Atmospheric Physics, Academy of Science, Prague, Bocni II/1401, 14131, Prague, Czech Republic. (dp@ufa.cas.cz)

conductivity of air near ground level and that the ensuing increase of current in the fair weather global circuit would lower the ionosphere. However, *Freund et al.* [2009] have demonstrated that even if radon is coming out of the ground in seismic areas, its contribution to the air conductivity is of minor importance relative to the air ionization rate which can be expected from charge carriers from the rocks. They have shown experimentally that these mobile electric charge carriers flow out of the stressed rocks [see *Freund et al.*, 2009, and references therein]. At the Earth's surface, these cause extra ionization of the air molecules. It has also been shown by *Kuo et al.* [2011] that ionospheric density variations can be induced by changes of the current in the global electric circuit between the bottom of the ionosphere and the Earth's surface where electric charges associated with stressed rocks can appear.

[3] A statistical study of the seismo-electromagnetic effects observed in the data from the French microsatellite DEMETER (Detection of Electro-Magnetic Emissions Transmitted from Earthquake Regions) is presented in this paper. The instrumentation used and the method of analysis are presented in section 2. Section 3 contains the observed results, and sections 4 and 5 are devoted to a discussion of the results and to the conclusions, respectively.

## 2. Data Set and Processing

[4] DEMETER (Detection of Electro-Magnetic Emissions Transmitted from Earthquake Regions) was a low-altitude satellite (altitude  $\sim 710$  km) launched in June 2004 into a circular polar orbit. The altitude of the satellite was decreased to  $\sim 660$  km in December 2005. The satellite science mission came to an end in December 2010, providing about 6.5 years of continuous data. The orbit of DEMETER was nearly Sun synchronous. The up-going half orbits corresponded to nighttime (22.30 LT), whereas the down-going half orbits corresponded to daytime (10.30 LT). Instruments aboard this satellite measured electromagnetic waves and plasma parameters all around the globe except in the auroral zones (geomagnetic latitudes  $>65^\circ$ ) [*Parrot et al.*, 2006]. Among all these instruments, we have focused only on wave electric field data. There were two different modes of operation of the satellite, called Burst and Survey. During the Burst mode, more detailed data were collected, but this mode was active only above limited (mostly seismically active) areas. As our study requires global data coverage, we used the low-resolution Survey mode data instead. The ICE (Instrument Champ Electrique) provides us, within the VLF range (20 Hz–20 kHz), which is the frequency range in which we are interested, with frequency spectra of one electric field component calculated on board with a frequency resolution of about 19.53 Hz and a time resolution of about 2 s. A more detailed description of the ICE instrument can be found in *Berthelier et al.* [2006]. We limit our analysis to the frequency range below 10 kHz in order to avoid the frequencies of man-made terrestrial VLF transmitters used for long-distance communications. Following *Němec et al.* [2008], we have selected 16 frequency bands (each with a bandwidth of  $\sim 117$  Hz) in such a way that they exclude spacecraft interferences and cover the entire frequency range studied as uniformly as possible. All the appropriate data recorded during the lifetime of the DEMETER mission, i.e.,

from September 2004 to December 2010, were included in the study.

[5] The US Geological Survey earthquake catalog (<http://earthquake.usgs.gov>) was used for the earthquake data. Altogether, about 12,000 earthquakes with magnitudes  $\geq 5.0$  occurred all over the world during the period analyzed. All of these were included in the study. Additional analysis was done using a larger data set of about 153,000 earthquakes with magnitude  $\geq 3$ .

[6] We used a modification of the data-processing method developed and described by *Němec et al.* [2008, 2009]. The basic idea of the method is to collect all available data observed in the vicinity of earthquakes and to interpret them in the context of long-term distributions obtained for similar ionospheric conditions. In the first step of the data processing, it is therefore necessary to describe the distribution of the intensities of electromagnetic waves observed by DEMETER using all of the available data. This long-term distribution of intensities is calculated separately for each combination of parameters, i.e., geomagnetic latitude and longitude, geomagnetic activity described by the  $Kp$  index, year, and season of the year. We constructed a multidimensional array with the number of dimensions equal to the number of parameters. In each bin of this array, we stored a histogram of the wave intensities observed during the appropriate ionospheric conditions. Each histogram represents a probability density function  $f(E)$ , where  $E$  is a power spectral density of the electric field fluctuations. The histograms were then used to calculate an experimental cumulative distribution function (CDF) of the wave intensity for each of the bins, using

$$F_i = \int_{-\infty}^{E_i} f(E) dE, \quad (1)$$

where  $E_i$  is the measured power spectral density. In the second step of the data processing, the data related to the earthquakes (i.e., the data acquired close to earthquake epicenters both in space and time) are considered. These data were evaluated using the CDFs obtained in the first step of the data processing, and it was determined whether they were different from the expected distributions for seismically unperturbed conditions. To do so, we organized the data related to earthquakes into a grid as a function of the frequency, the time relative to the main shock (2 days before and 1 day after, with a resolution of 4 h), and the distance of the satellite footprint from the earthquake epicenter up to 440 km (resolution 110 km). We have analyzed both daytime and nighttime data from the entire lifetime of the DEMETER mission [*Piša et al.*, 2012]. The daytime data show no significant effect, probably because the ionospheric conditions are generally more disturbed and then the detection of seismo-electromagnetic effects is less likely. In this paper, we will therefore focus only on the nighttime data. Data belonging to more than one earthquake (typically the main shock and aftershocks) were excluded from the analysis in order to avoid the mixing of preseismic and postseismic activity. Otherwise, a single measurement might be used more than once, and it would be impossible to specify to which earthquake the observed data should be attributed. This condition reduces the number of earthquakes considered to  $\sim 8400$  events. The corresponding CDF was evaluated for each measurement using the results of the above described first step

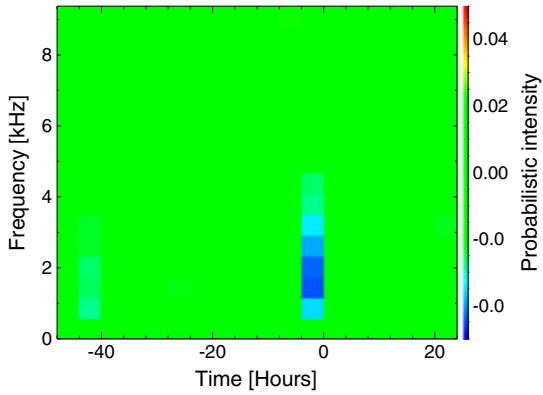


**Figure 1.** Frequency-time dependence of the probabilistic intensity (see text) obtained from the nighttime electric field data measured within 440 km of the epicenters of earthquakes with magnitudes  $\geq 5.0$ .

of our analysis. In this way, we obtain a large set of values which, in the absence of seismic influences, should be uniformly distributed between 0 and 1. Afterwards, we define a probabilistic intensity  $I$  in each bin of the grid as a mean value of the CDFs in a given bin. Namely, for a bin  $b$ ,

$$I_b = \frac{\sum_{i=1}^{M_b} F_i}{M_b}, \quad (2)$$

where  $M_b$  is the number of cumulative probabilities  $F_i$  collected in a given bin  $b$ . According to the central limit theorem, the values of the probabilistic intensity should approximately follow the normal distribution with a mean value of 0.5. The value 0.5 is therefore subtracted to obtain a mean value equal to 0. Values lower than 0 mean that the emissions in a given bin are less intense than normal, while values larger than 0 mean that the emissions in a given bin are more intense than normal.

### 3. Results

[7] We have parameterized the background activity with a different set of parameters, compared to *Němec et al.* [2008, 2009] and *Piša et al.* [2012]. The main aim was to characterize the natural seasonal and annual variations of VLF wave intensity more precisely. We use a moving frame of 3 months (December–February, March–May, June–August, September–November) covering the complete DEMETER mission. On the other hand, we parameterize the geomagnetic activity, reflecting the solar wind input and the magnetospheric response, by the  $Kp$  index, in a reduced set of two bands ( $<3\sigma$ ;  $\geq 3\sigma$ ). We have also increased the resolution of the wave intensity to 160 bins between  $10^{-4}$  and  $10^4 \mu\text{V}^2\text{m}^{-2}\text{Hz}^{-1}$  equidistantly distributed in a logarithmic scale, to enable a more detailed inspection of the wave intensity variation. In the contrast with a previous analysis, we have ensured that for each relevant earthquake, the same amount of data contributes to the individual time bin. For each earthquake, only eight values closest to the epicenter were selected. Given the time resolution of the measurements and the spacecraft orbital velocity, these eight values approximately correspond to a spatial scale of 100 km (calculated from the time resolution and satellite velocity). The idea

is to select the same amount of data for each contributing earthquake in a given temporal bin.

[8] Figure 1 shows the frequency-time dependence of the probabilistic intensity obtained for distances  $<440$  km from the epicenter of earthquakes with magnitudes  $\geq 5$ . The minimum of probabilistic intensity is observed at frequencies of about 1.7 kHz shortly (0–4 h) before the time of the main shock. The minimum value of the probabilistic intensity is equal to about  $-0.044$ . It corresponds to an attenuation of wave intensity by about 2 dB. This means that the decrease of wave intensity related to the seismic activity is rather small as compared to normal variations of about  $\pm 7.5$  dB.

[9] This attenuation is small but, taking into account the large volume of data, it can still be statistically significant. To evaluate its significance, only the data measured shortly (0–4 h) before the times of the main shocks at distances  $<440$  km from the earthquake epicenters and at frequencies of about 1.7 kHz have been used. The total number of 2952 values (369 earthquakes) has been analyzed. We have normalized the appropriate mean value by its standard deviation. The standard deviation has been estimated by taking into account the uniform distribution of the cumulative distribution values and by assuming that all of these values are independent. As this is not exactly the case, the upper estimate of standard deviation based on the number of individual half orbits that can be considered as independent has been used. This upper estimate can be then calculated for each time bin as

$$\sigma = \frac{1}{\sqrt{12N}}, \quad (3)$$

where  $N$  is the number of individual half orbits. Figure 2 presents the probabilistic intensity obtained in the time interval 0–4 h (black line) and 24–28 h (gray line) before the times of the main shocks at frequencies of about 1.7 kHz as a function of the number of analyzed earthquakes; these are accumulated from July 2004 to December 2010. The dates by which the given numbers of earthquakes have been

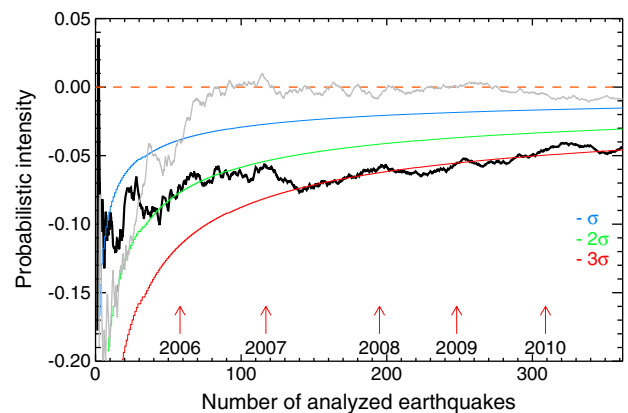


**Figure 2.** Probabilistic intensity obtained in the time interval 0–4 h (black line) and 24–28 h (gray line) before the times of the main shocks at frequencies of about 1.7 kHz as a function of the number of accumulated independent earthquakes during the DEMETER mission. Blue, green, and red lines, respectively, show  $1\sigma$ ,  $2\sigma$ , and  $3\sigma$  levels of the statistical significance (see equation 3). The dashed orange line represents the probabilistic intensity equals to zero.

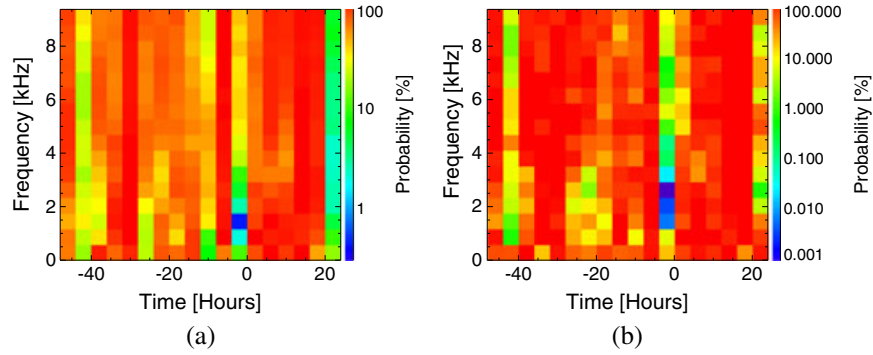


**Figure 3.** Time-frequency dependence of the probability of random occurrence of results using (a) the classical  $t$  test and (b) the binomial distribution. A more detailed explanation is given in the text.

accumulated are shown on the bottom. Three different levels of statistical significance are represented by the colored lines:  $\sigma$  (blue),  $2\sigma$  (green), and  $3\sigma$  (red). The decrease of probabilistic intensity measured in the time interval 0–4 h below zero tends to the  $3\sigma$  significance level after  $\sim 125$  analyzed earthquakes, and then oscillates around that level. A value of the normalized probabilistic intensity calculated using the whole available data set of 362 independent earthquakes corresponds to about  $-2.9$  standard deviations. The statistical significance of this result is very high, with the probability of it arising by chance being only  $\sim 0.3\%$ , assuming that the values obtained conform to a normal distribution of obtained values. The probabilistic intensity obtained in the time interval 24–28 h before the main shocks fluctuates

above  $1\sigma$  significance and corresponds to a situation of no seismic-related effect. Figure 2 also shows that the probabilistic intensity corresponding to the effect was slightly increasing for the number of earthquakes larger than 150. This may explain why *Němec et al.* [2008, 2009] and *Piša et al.* [2012] have reported lower values of probabilistic intensity. Nevertheless, the effect is always observed at the same time and frequency.

[10] To verify these results, the significance can now be evaluated not only for the strongest effect but for all the time-frequency variations of the probabilistic intensity shown in Figure 1. Two different methods are used. First, we use the classical  $t$  test [Press et al., 1992]. The results obtained are shown in Figure 3a. This is a statistical test designed

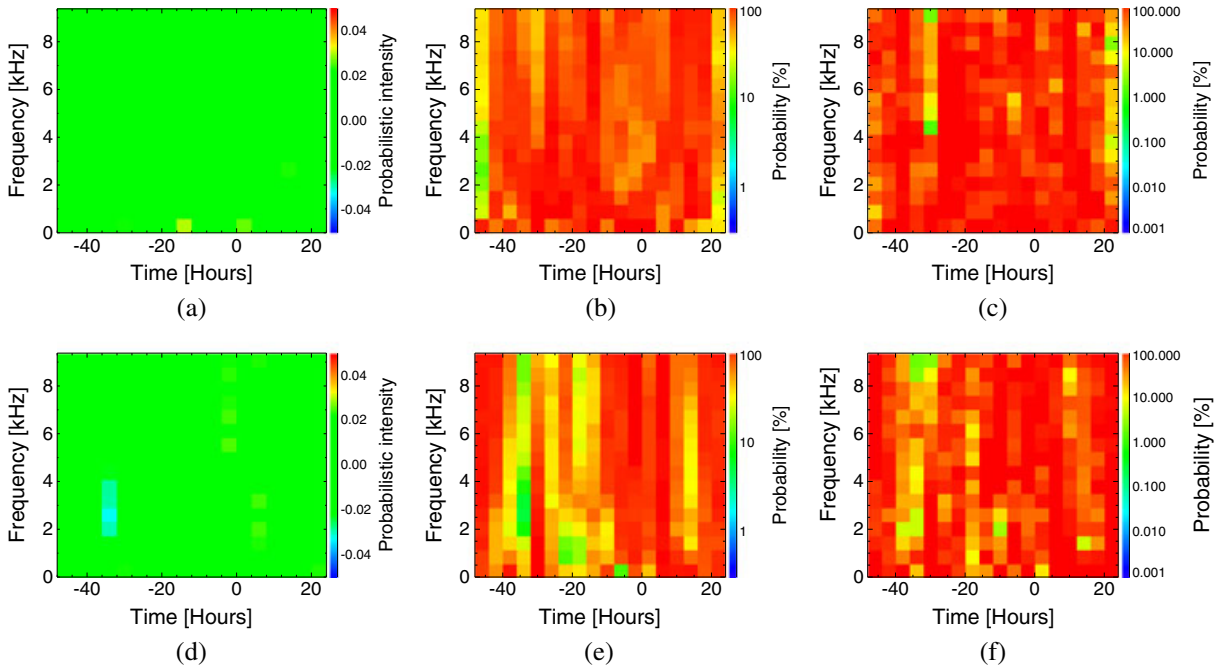


**Figure 4.** Time-frequency dependence of the probabilistic intensity (a) for earthquakes with the time of the main shocks shifted 10 days into the past and (d) for earthquakes with positions shifted  $25^\circ$  westward. Time-frequency dependence of the probability of random occurrence of results calculated using the classical  $t$  test (b) for earthquakes with the time of the main shocks shifted 10 days into the past and (e) for earthquakes with positions shifted  $25^\circ$  westward. Time-frequency dependence of the probability of random occurrence of results calculated using the binomial distribution (c) for earthquakes with the time of the main shocks shifted 10 days into the past and (f) for earthquakes with positions shifted  $25^\circ$  westward.

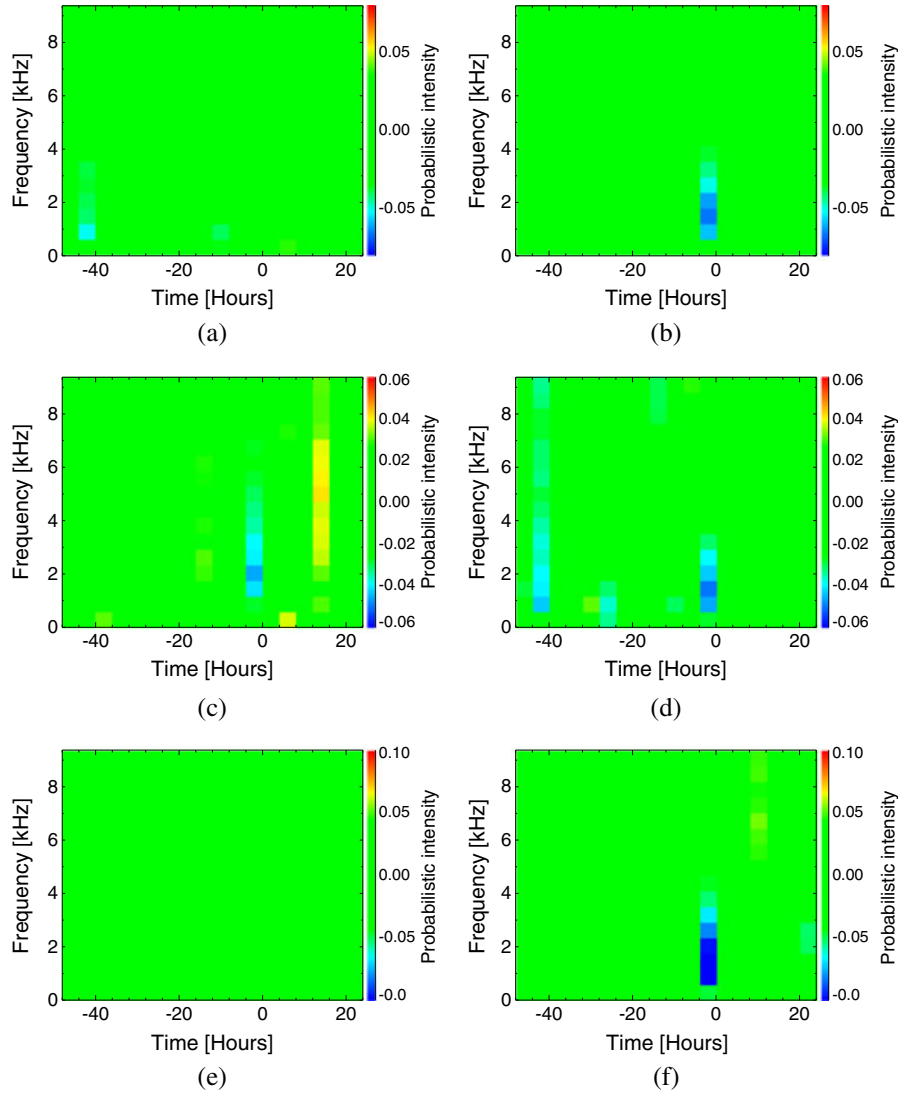


**Figure 5.** Frequency-time dependencies of the probabilistic intensity obtained for the nighttime electric field data measured within 440 km from the epicenters of earthquakes with magnitudes  $\geq 5.0$  for the seasons (a) between September and February and (b) between March and August; positions with geomagnetic latitudes (c)  $\leq 20^\circ$  and (d)  $> 20^\circ$ ; and hypocenters located (e) below land and (f) below the sea.

to assess whether the means of two normally distributed populations are equal. We have tested the possibility that the observed deviation of the mean from 0 is random (0 is the expected mean value if no seismic-related effects were present). The resulting probability in the time interval 0–4 h before the times of the main shocks and at frequencies of 1.7 kHz is about 0.5%, which again means that the observed deviation of the mean value from 0 is unlikely to be random. The probability is by at least 1–2 orders of magnitude larger in all other time-frequency bins. The second method that we use to estimate the statistical significance of the observed effect is to determine the number of values corresponding to a decrease of wave intensity and the number of values corresponding to an increase of wave intensity. The probability that such a situation might occur randomly was then evaluated using a binomial distribution with the anticipated probability of a decrease being equal to the

anticipated probability of an increase. The results obtained are shown in Figure 3b. The numbers of values corresponding to a decrease of wave intensity (221) and the number of values corresponding to an increase of wave intensity (148) have been counted for data measured in time intervals 0–4 h before the times of the main shocks, and at frequencies of about 1.7 kHz. The probability that the result might occur by chance is only about 0.001%, which again means that the observed decrease of VLF wave intensity is highly unlikely to be random. Again, this probability is much higher in all other time-frequency bins. Note that this test gives the strongest effect at slightly higher frequencies (around 3 kHz), because at these frequencies, the decreases of the probabilistic intensity are observed more often, but they are weaker than at 1.7 kHz.

[11] On top of the tests of the statistical significance, we have used two additional tests for the reliability of the

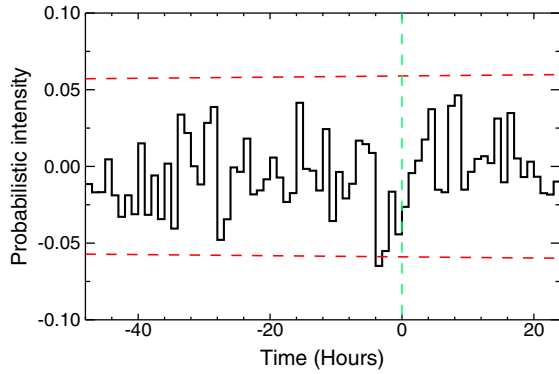


**Figure 6.** The probabilistic intensity obtained between 2 days before and 1 day after the times of the main shocks at frequencies of about 1.7 kHz with 1 h resolution. Significance levels equal to  $\pm 2\sigma$  are represented by dashed red lines. The dashed green line shows the time of the main shock.

obtained results. Two different control sets, consisting of modified earthquake data have been used. First, we have used a set of earthquakes with the times of the main shocks artificially shifted 10 days to the past. Then we have used a set of earthquakes with the positions of the epicenters artificially shifted  $25^\circ$  westward which is the distance between two neighboring half orbits. Figure 4 shows the results. The color scales are the same as in the original plots (Figures 1 and 3). It can be seen in Figures 4a and 4d that the analysis of these control sets does not display any particular variation of the probabilistic intensity. This is further confirmed by the tests of statistical significance, which show that the observed fluctuations of probabilistic intensity are likely to be caused by random variations. In Figure 4b and 4e, there are no blue portions as there are in Figure 3a; similarly, in Figures 4c and 4f, there are no blue parts as in Figure 3b.

[12] Having demonstrated the existence of a definite seismic-related decrease of 1.7 kHz wave intensity shortly (0–4 h) before the times of the main shocks, we continue by investigating possible controlling parameters, i.e., we try to determine under which conditions the effect is strongest. The time–frequency dependence of the probabilistic intensity is shown in Figure 5 for two different seasons: (a) September–February and (b) March–August. Again, all available data measured within 440 km of earthquakes with magnitudes  $\geq 5$  were used. The probabilistic intensity in the time bin 0–4 h before the times of the main shocks and at frequencies of about 1.7 kHz is equal to  $-0.019$  for the season between September and February, while it is  $-0.067$  for the season between March and August. This apparent seasonal variation correlates with the seasonal variation of lightning activity, which is on average globally larger between March and August [Christian *et al.*, 2003].

[13] Next, we have calculated the probabilistic intensity taking into account satellite measurements of at geomagnetic latitudes  $\leq 20^\circ$ , and geomagnetic latitudes  $>20^\circ$  shown in Figures 5c–5d. The limit of  $20^\circ$  was set in order to obtain two data sets of about the same size. The results obtained for the time interval 0–4 h before the times of the main shocks and at frequencies of about 1.7 kHz show that the probabilistic intensity is equal to  $-0.041$  for geomagnetic latitudes

$\leq 20^\circ$  while it is equal to  $-0.050$  for geomagnetic latitudes  $>20^\circ$ . This may be taken to be in agreement with the results of Němec *et al.* [2010], when the VLF waves intensity is higher for higher geomagnetic latitudes.

[14] Then, we have divided the data into two groups, depending on whether the hypocenter of the relevant earthquake was located below the sea or below land. The resulting value of the probabilistic intensity obtained for the time interval 0–4 h before the times of the main shocks and at frequencies of about 1.7 kHz is equal to  $-0.109$  for earthquake hypocenters below the sea, while for positions below land, it is  $-0.018$ . Thus, the effect is stronger for earthquakes with hypocenters below the sea than for earthquakes with hypocenters below land. This dependence can be explained by the lower attenuation of VLF waves propagating in the Earth–ionosphere waveguide above the sea [e.g., Meyer *et al.*, 2011]. The factor which plays a significant role is the conductivity of the surface of the lower boundary of the waveguide.

[15] Concerning the dependence on the depth of hypocenters (not shown), the probabilistic intensity is equal to about  $-0.059$  for the depth  $<33$  km while it is equal to about  $-0.032$  for the depth  $\geq 33$  km. The effect is stronger for shallow earthquakes than for deeper ones. However, the results may be biased by the effects of analysis: if it is not possible to determine the depth of a hypocenter, then its value is artificially set to 10 km.

[16] The most extreme value of probabilistic intensity is always observed shortly (0–4 h) before the times of the main shocks. Can the effect be attributed to a preseismic activity or is it more likely to be related to the main shock? The dependence of the probabilistic intensity as a function of time relative to the times of the main shocks at frequencies of about 1.7 kHz obtained for distances  $< 440$  km from the epicenters of earthquakes is presented in Figure 6. The time resolution is 1 h. Dashed red lines represent significance levels equal to  $\pm 2\sigma$ . It can be seen that the probabilistic intensity which normally fluctuates between  $\pm 2\sigma$ , decreases 3–4 h before the time of the main shock to less than  $-2\sigma$ . There are about 90 events included in each of the bins. The decrease at 3–4 h before the time of the main shock is formed

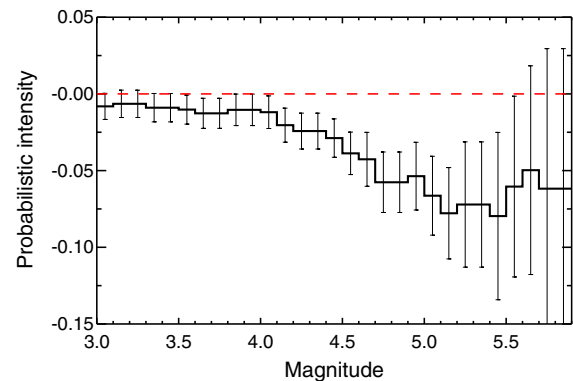


**Figure 7.** Probabilistic intensity obtained in the time interval 0–4 h before the times of the main shocks at frequencies of about 1.7 kHz as a function of increasing thresholds of earthquake magnitude. The error bars correspond to upper estimates of standard deviations (see text). Dashed red line represents the probabilistic intensity equal to 0 (see text).

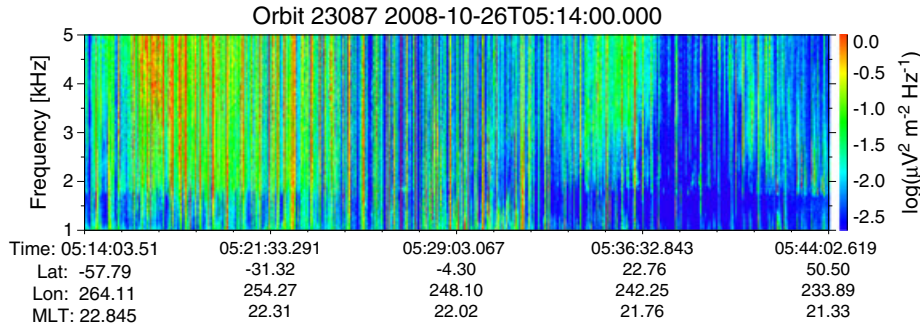


**Figure 8.** Frequency-time spectrogram of the power spectral density of electric field fluctuations observed by DEMETER on 26 October 2008 between 05:14 and 05:44 UT . Note the whistler cutoff frequency of the whistlers (vertical lines) at about 1.7 kHz. The cutoff frequency remains nearly constant at all of the sampled latitudes.

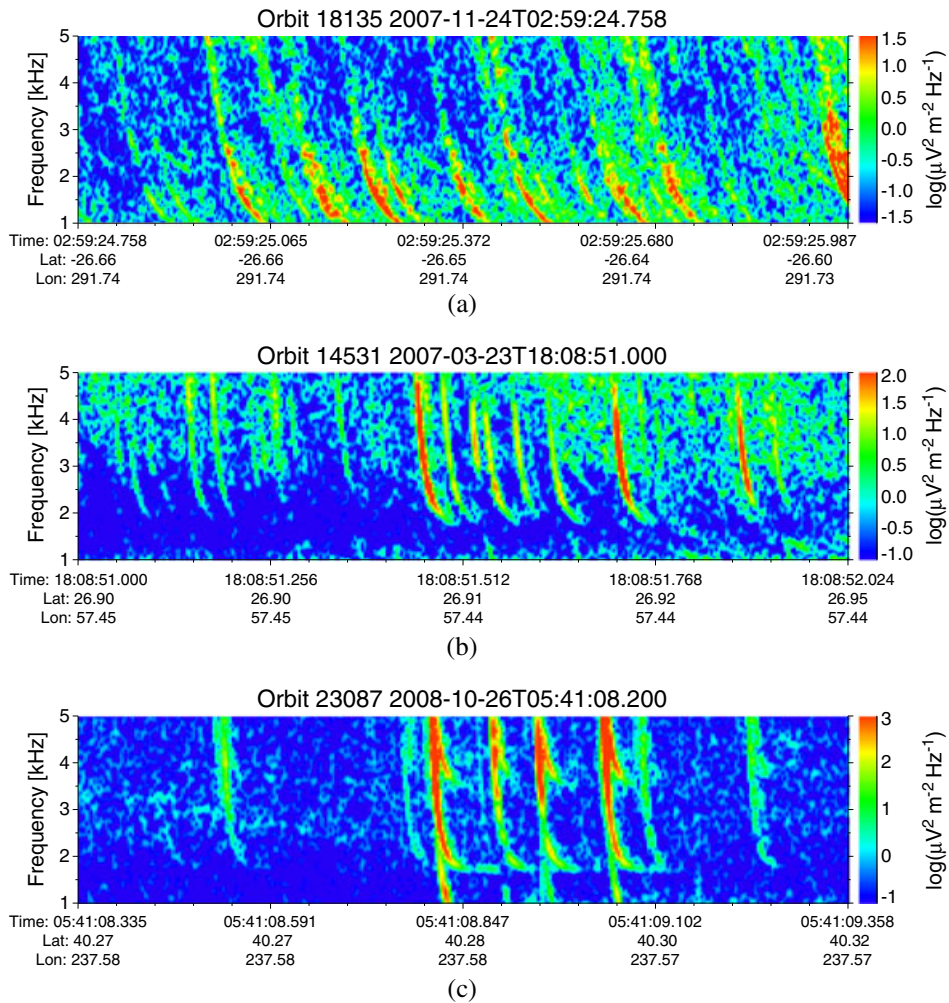


**Figure 9.** Frequency-time spectrograms of the power spectral density of electric field fluctuations measured in the Burst mode for typical whistler wave signatures. (a) Broadband signal of the fractional hop whistlers from about 1 to 5 kHz with no Earth-ionosphere waveguide cutoff present measured on 24 November 2007. (b) Fractional hop whistler with a cutoff at about 1.7 kHz observed on March 23, 2007. (c) The cutoff frequencies of the fractional hop whistlers at about 1.7 and 3.4 kHz observed on 26 October 2008.



by 600 data points coming from 75 different events. The mean value of probabilistic intensity in this bin is  $-0.065$ , corresponding to a decrease of wave intensity equal to about 2.3 dB. The decrease is statistically significant at the 95% level. The results show that the obtained effect is unlikely to be attributed to coseismic activity.

[17] We have also analyzed a possible influence of earthquake magnitude on the effect. We have again used the data measured shortly (0–4 h) before the times of the main shocks at distances  $<440$  km from the earthquake epicenters and at frequencies of about 1.7 kHz. However, we have lowered the magnitude threshold down to the earthquake magnitude  $\geq 3.0$  in order to be able to analyze the dependence over a larger range of magnitudes. We have applied the rule for selection of data (to avoid measurements that occurred close to more than one earthquake—see section 2) with this lower magnitude. This selection procedure leads to removing more data from the analysis compared to the case when the selection is done for higher magnitudes. However, it represents the only possibility for doing the analysis consistently on the same data set for different magnitude thresholds. The results are shown in Figure 7. The horizontal axis represents a magnitude threshold: all events with magnitudes larger than or equal to this threshold have been used in the analysis. The red line represents the probabilistic intensity equal to 0, i.e., the value expected if no seismic-related effects were present. Values lower than 0 mean that the emissions are less intense than normal, while values larger than 0 mean that the emissions are more intense than normal. There is a clear correlation between the earthquake magnitude and the strength of the observed effect, with an obvious magnitude threshold of  $M 4$  required for the effect to occur. The effect seems to increase with the earthquake magnitude. At the largest magnitudes, above  $M 5.5$ , the number of analyzed data rapidly decreases and hence the uncertainty of the results increases and starts to mask possible effects.

#### 4. Discussion

[18] As noted in recent studies [e.g., Harrison *et al.*, 2010], the frequency of about 1.7 kHz where the decrease of wave intensity was observed corresponds approximately to the low-frequency cutoff for propagation in the Earth-ionosphere waveguide at night [Budden, 1961]. This frequency is inversely proportional to the height of the lower boundary of the ionosphere. Taking into account that the electromagnetic waves generated by lightning in thunderstorms are a crucial source of VLF radiation observed by DEMETER during the nighttime [Němec *et al.*, 2010], it can be expected that the exact frequency of this cutoff can significantly affect the power spectrum of electromagnetic waves observed by DEMETER at frequencies of about 1.7 kHz. This is well illustrated in Figure 8, which shows an example of the frequency-time spectrogram of power spectral densities (PSD) of electric field fluctuations observed during one nighttime DEMETER half orbit in the time interval 0–4 h before the main shock. The frequency cutoff at a frequency of about 1.7 kHz can be clearly identified as the frequency below which the power spectral density of the electric field fluctuations drastically decreases. This example is related to an earthquake with magnitude 5.0 that occurred on 26

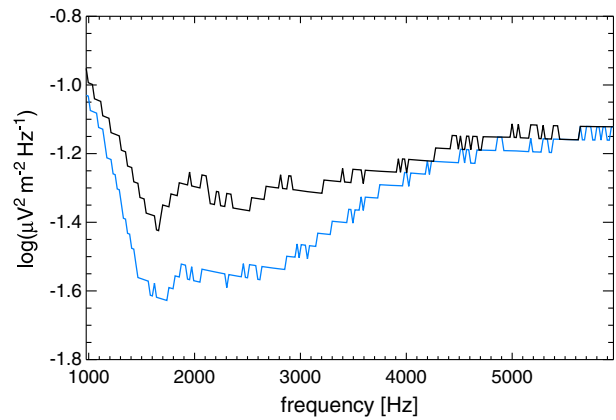


**Figure 10.** Median frequency spectrum of PSD of electric field fluctuations obtained for the nighttime electric field data measured within 440 km from the epicenters of earthquakes with magnitudes  $\geq 5.0$ . The results obtained for data measured 0–4 hours before the times of the main shocks are shown in blue, while the results obtained for data measured 24–28 hours before times of the main shocks are shown in black.

October 2008 at 09:27:22 UT. The epicenter was located at  $40.34^\circ\text{N}$ ,  $124.63^\circ\text{W}$ , and the depth of hypocenter was 21 km.

[19] We have checked all burst mode data measured in the time interval 0–4 h before the times of the main shocks at distances less than 440 km from earthquake epicenters. For each of the 70 events, we have calculated a detailed frequency-time spectrogram of the power spectral density (note that a waveform of one electric field component was measured in the Burst mode, so that frequency-time spectrograms with sufficient frequency and time resolutions are available). Whistler wave activity originating from lightning strokes has been observed for all the analyzed events. These lightning-originating electromagnetic waves are found to be the most intense waves in the frequency range of interest ( $\sim 1.7$  kHz) during the night. Three typical whistler wave signatures were as follows: (1) When the satellite is almost above a lightning flash, a broadband signal from about 1 to 5 kHz is observed. It means that there is no Earth-ionosphere waveguide cutoff present in this case, shown for 1 s of data in Figure 9a. (2) When the satellite is further from the flash, a fractional hop whistler with a cutoff at about 1.7 kHz is observed, see Figure 9b, or (3) fractional hop whistlers are observed with dispersion signatures and partial or total cutoffs at 1.7 and 3.4 kHz, see Figure 9c.

[20] The height of the lower boundary of the ionosphere exhibits a seasonal variation, and it also depends on the position of observation [Toledo-Redondo *et al.*, 2012]. It is therefore hard to compare observations of absolute values of VLF wave intensity, which depend on the positions and on season. Nevertheless, we selected earthquakes for which data measured within 440 km of earthquake epicenters 0–4 h and 24–28 h before the times of the main shocks were available. We have visually checked the earthquake orbits for the presence of changes in the cutoff frequency. However, no clear change in the cutoff frequency was identified. Nevertheless, the variations of the cutoff frequency can be identified by analyzing a larger number of events. Figure 10 shows the corresponding median spectra. These spectra were

calculated using all available data for the time interval 0–4 h (blue line) and 24–28 h (black line). Altogether, more than 2000 spectra from 58 earthquakes ( $M \geq 5$ ) were used. It can be seen that the wave intensity at frequencies between about 1.5 and 4.0 kHz is lower at times shortly (0–4 h) before the times of the main shocks (blue line) than more than one day before the times of the main shocks. The frequency of the minimum wave intensity is slightly shifted from about 1.66 kHz (black line) to 1.73 kHz (blue line). Nevertheless, it is necessary to keep in mind that the wave intensity is very variable, and that the number of events taken into account is quite small. However, this result clearly demonstrates the additional attenuation of wave intensity shortly (0–4 h) before the times of the main shocks.

[21] The observed dependence of the effect on geomagnetic latitude, on the positions of the hypocenters and on the season of the year appears to be consistent with the suggested explanation based on the attenuation of electromagnetic waves caused by lightning propagating in the Earth-ionosphere waveguide.

## 5. Conclusions

[22] We have presented a detailed analysis of a previously reported decrease of electromagnetic wave intensity observed by the DEMETER spacecraft at frequencies of about 1.7 kHz in the vicinity of imminent earthquakes [Němec et al., 2008, 2009; Piša et al., 2012]. We have used all of the nighttime data collected during the DEMETER mission ( $\sim 6.5$  years). We confirm the existence of a weak, but statistically significant (at 2.3 standard deviations), decrease of wave intensity observed within 440 km from the epicenters of earthquakes with the magnitudes  $\geq 5$  shortly (0–4 h) before the times of the main shocks. Two statistical tests and the analysis of two control data sets show that the observed effect is unlikely to be due to chance. Our results also show that the effect is stronger: (i) during the most active thunderstorm season (March–August); (ii) at higher geomagnetic latitudes; (iii) for earthquakes with hypocenters below the sea; and (iv) for shallower earthquakes ( $< 33$  km).

[23] This effect could result from an increase in the electric conductivity of the lower troposphere possibly due to an increase of charge carriers emanating from the stressed rocks prior to a major earthquake. This causes the air conductivity to increase; the electric current down from the ionosphere also increases, by Ohm's law [Rycroft and Harrison, 2012], which manifests itself as a slight lowering of the nighttime ionosphere, at about 88 km, by  $\sim 2$  km [Harrison et al., 2010]. Therefore, VLF radio waves originating from lightning and propagating in the Earth-ionosphere waveguide at night are cut off at a slightly higher frequency than usual, 1.74 kHz rather than 1.70 kHz. This means that there is additional attenuation of signals from lightning propagating in the Earth-ionosphere waveguide, so that the intensity of fractional hop whistlers received at DEMETER is less than usual. It is important to note that this effect is very small (a decrease of  $\sim 2$  dB), as compared to usual variations in the background activity ( $\pm 7.5$  dB), and it will therefore be very difficult to observe it directly in individual cases. A large number of events ( $> 1000$ ) is necessary to show a statistically significant ( $> 2\sigma$ ) effect; this has been clearly demonstrated here.

[24] **Acknowledgments.** This work was supported by the Centre National d'Etudes Spatiales. It is based on observations with the electric instrument ICE aboard DEMETER. The authors thank J. J. Berthelier, the PI of this instrument, for the use of the data. Part of the studies leading to these results was funded from the European Community Seventh Framework Programme (FP7/2007–2013), under grant agreement 262005. This work was also supported by the Academy of Science of the Czech Republic under grant M100431206. FN acknowledges support from grant P209-12-P658. DP and OS acknowledge support from grant P209-11-2280 and 205-09-1253.

[25] Robert Lysak thanks Jan Blecki and Friedemann Freund for their assistance in evaluating this paper.

## References

- Asada, T., H. Baba, M. Kawazoe, and M. Sugiura (2001), An attempt to delineate very low frequency electromagnetic signals associated with earthquakes, *Earth Planets Space*, *53*, 55–62.
- Berthelier, J.-J., et al. (2006), ICE the electric field experiment on DEMETER, *Planet. and Space Sci. Elsevier*, *54*, 456–471.
- Bortnik, J., J. W. Cutler, C. Dunson, and T. E. Bleier (2008), The possible statistical relation of Pc1 260 pulsations to Earthquake occurrence at low latitudes, *Ann. Geophys.*, *26*, 2825–2836.
- Budden, K. G. (1961), *The Waveguide Mode Theory of Wave Propagation*, Prentice-Hall, Englewood Cliffs, N.J.
- Christian, H. J., et al. (2003), Global frequency and distribution of lightning as observed from space by the Optical Transient Detector, *J. Geophys. Res.*, *108*, doi:10.1029/2002JD002347, in press.
- Chilverd, M. A., C. J. Rodger, and N. R. Thomson (1999), Investigating seismo-ionospheric effects on a long subionospheric path, *J. Geophys. Res.*, *28*, 28,171–28,179.
- Freund, F. (2011), Pre-earthquake signals: Underlying physical processes, *J. of Asian Earth Sci.*, *41*, 383–400.
- Freund, F. T., I. G. Kulauci, G. Cyr, J. Ling, M. Winnick, J. Tregloan-Reed, and M. M. Freund (2009), Air ionization at rock surfaces and pre-earthquake signals, *J. Atmos. Sol. Terr. Phys.*, *71*(17–18), 1824–1834, doi:10.1016/j.jastp.2009.07.013.
- Harrison, R. G., K. L. Aplin, and M. J. Rycroft (2010), Atmospheric electricity coupling between earthquake regions and the ionosphere, *J. Atmos. Sol. Terr. Phys.*, *72*, 376–381.
- Hattori, K. (2004), ULF geomagnetic changes associated with large earthquakes, *Terr. Atmos. Oceanic Sci.*, *15*, 329–360.
- Henderson, T. R., V. S. Sonwalkar, R. A. Helliwell, U. S. Inan, and A. C. Fraser-Smith (1993), A search for ELF/VLF emissions induced by earthquakes as observed in the ionosphere by the DE-2 satellite, *J. Geophys. Res.*, *98*, 9503–9514.
- Hobara, Y., and M. Parrot (2005), Ionospheric perturbations linked to a very powerful seismic event, *J. Atmos. Sol. Terr. Phys.*, *67*, 677–685.
- Kon, S., M. Nishihaishi, and K. Hattori (2011), Ionospheric anomalies possibly associated with  $M \geq 6.0$  earthquakes in the Japan area during 1998–2010: Case studies and statistical study, *J. Asian Earth Sci.*, *41*, 410–420.
- Kuo, C. L., J. Huba, G. Joyce, and L. Lee (2011), Ionosphere plasma bubbles and density variations induced by pre-earthquake rock currents and associated surface charges, *J. Geophys. Res.*, *116*, A10317, doi:10.1029/2011JA016628.
- Larkina, V. I., V. V. Migulin, O. A. Molchanov, I. P. Kharkov, A. S. Inchin, and V. B. Schvetcova (1989), Some statistical results on very low frequency radiowave emissions in the upper ionosphere over earthquake zones, *Phys. Earth Planet. Inter.*, *57*, 100–109.
- Liu, J. Y., Y. B. Tsai, S. W. Chen, C. P. Lee, Y. C. Chen, H. Y. Yen, W. Y. Chang, and C. Liu (2006), Giant ionospheric disturbances excited by the M9.3 Sumatra earthquake of 26 December 2004, *Geophys. Res. Lett.*, *33*, doi:10.1029/2005GL023963, in press.
- Meyer, S. G., A. B. Collier, and C. J. Rodger (2011), Daytime VLF modeling over land and sea, comparison with data from DEMETER satellite, *IEEE Conference publications, General Assembly and Scientific Symposium, 2011 XXXth URSI*, doi:10.1109/URSIGASS.2011.6051108, in press.
- Molchanov, O. A., O. A. Mazhaeva, A. N. Goliavin, and M. Hayakawa (1993), Observation by the Intercosmos-24 satellite of ELF–VLF electromagnetic emissions associated with earthquakes, *Ann. Geophys.*, *11*, 431–440.
- Němec, F., O. Santolík, M. Parrot, and J. J. Berthelier (2008), Spacecraft observations of electromagnetic perturbations connected with seismic activity, *Geophys. Res. Lett.*, *35*, doi:10.1029/2007GL032517, in press.
- Němec, F., O. Santolík, and M. Parrot (2009), Decrease of intensity of ELF/VLF waves observed in the upper ionosphere close to earthquakes:

- A statistical study, *J. Geophys. Res.*, 114, doi:10.1029/2008JA013972, in press.
- Němec, F., O. Santolík, M. Parrot, and C. J. Rodger (2010), Relationship between median intensities of electromagnetic emissions in the VLF range and lightning activity, *J. Geophys. Res.*, 115, doi:10.1029/2010JA015296.
- Parrot, M. (1994a), Statistical study of ELF/VLF emissions recorded by a low-altitude satellite during seismic events, *J. Geophys. Res.*, 99, 23,339–23,347.
- Parrot, M. (1994b), Seismo-electromagnetic waves detected by a low-altitude satellites, in *Electromagnetic Phenomena Related to Earthquake Prediction*, edited by V. Hayakawa and Y. Fujinawa, pp. 361–372, Terra Scientific, Tokyo, Japan.
- Parrot, M., et al. (2006), The magnetic field experiment IMSC and its data processing onboard DEMETER: Scientific objectives, description and first results, *Planet. Space Sci.*, 54(5), 441–455.
- Píša, D., F. Němec, M. Parrot, and O. Santolík (2012), Attenuation of electromagnetic waves at the frequency  $\sim 1.7$  kHz in the upper ionosphere observed by the DEMETER satellite in the vicinity of earthquakes, *Annals of Geophys.*, 55, 157–163.
- Press, W. H., S. A. Teukolsky, W. T. Vetterling, and B. P. Flannery (1992), *Numerical Recipes in C. The Art of Scientific Computing*, 2nd ed., Cambridge Univ. Press, Cambridge, U.K.
- Pulinets, S. A., and K. A. Boyarchuk (2004), *Ionospheric Precursors of Earthquakes*, Springer, Heidelberg, New York.
- Rodger, C. J., N. R. Thomson, and R. L. Dowden (1996), A search for ELF/VLF activity associated with earthquakes using ISIS satellite data, *J. Geophys. Res.*, 101, 13,369–13,378.
- Rycroft, M., and R. Harrison (2012), Electromagnetic atmosphere-plasma coupling: The global atmospheric electric circuit, *Space Sci. Rev.*, 168, 363–384, doi:10.1007/s11214-011-9830-8.
- Serebryakova, O. N., S. V. Bilichenko, V. M. Chmyrev, M. Parrot, L. Rauch, F. Lefeuvre, and O. A. Pokhotelov (1992), Electrodynamical ELF radiation from earthquake regions as observed by low-altitude satellites, *Geophys. Res. Lett.*, 19, 91–94.
- Sorokin, V. M., V. M. Chmyrev, and A. K. Yaschenko (2001), Electrodynamic model of the lower atmosphere and the ionosphere coupling, *J. Atmos. Sol. Terr. Phys.*, 63, 1681–1691.
- Tate, J., and W. Daily (1989), Evidence of electro-seismic phenomena, *Phys. Earth Planet. Inter.*, 57, 1–10.
- Thomas, J. N., J. J. Love, and M. J. S. Johnston (2009a), On the reported magnetic precursor of the 1989 Loma Prieta earthquake, *Phys. Earth Planet. Inter.*, 173, 207–215, doi:10.1016/j.pepi.2008.11.014.
- Thomas, J. N., J. J. Love, M. J. S. Johnston, and K. Yumoto (2009b), On the reported magnetic precursor of the 1993 Guam earthquake, *Geophys. Res. Lett.*, 36, L16301, doi:10.1029/2009GL039020.
- Toledo-Redondo, S., M. Parrot, and A. Salinas (2012), Variation of the first cut-off frequency of the Earth-ionosphere waveguide observed by DEMETER, *J. Geophys. Res.*, 117, A04321, doi:10.1029/2011JA017400.